



# CHORUS

This is the accepted manuscript made available via CHORUS. The article has been published as:

## Strong Field Molecular Ionization in the Impulsive Limit: Freezing Vibrations with Short Pulses

Péter Sándor, Vincent Tagliamonti, Arthur Zhao, Tamás Rozgonyi, Matthias Ruckebauer,  
Philipp Marquetand, and Thomas Weinacht

Phys. Rev. Lett. **116**, 063002 — Published 9 February 2016

DOI: [10.1103/PhysRevLett.116.063002](https://doi.org/10.1103/PhysRevLett.116.063002)

# Strong Field Molecular Ionization in the Impulsive Limit: Freezing Vibrations with Short Pulses

Péter Sándor,<sup>1</sup> Vincent Tagliamonti,<sup>1</sup> Arthur Zhao,<sup>1</sup> Thomas Weinacht,<sup>1</sup>  
Tamás Rozgonyi,<sup>2</sup> Matthias Ruckebauer,<sup>3</sup> and Philipp Marquetand<sup>3</sup>

<sup>1</sup>*Department of Physics and Astronomy, Stony Brook University, Stony Brook NY 11794-3800*

<sup>2</sup>*Institute of Materials and Environmental Chemistry,*

*Research Centre for Natural Sciences, Hungarian Academy of Sciences,*

*Budapest 1117 Magyar tudósok krt. 2, Hungary*

<sup>3</sup>*University of Vienna, Faculty of Chemistry, Institute of Theoretical Chemistry, Währinger Str. 17, 1090 Wien, Austria*

(Dated: December 28, 2015)

We study strong-field molecular ionization as a function of pulse duration. Experimental measurements of the photoelectron yield for a number of molecules reveal competition between different ionization continua (cationic states) which depends strongly on pulse duration. Surprisingly, in the limit of short pulse duration, we find that a single ionic continuum dominates the yield, whereas multiple continua are produced for longer pulses. Using calculations which take vibrational dynamics into account, we interpret our results in terms of nuclear motion and non-adiabatic dynamics during the ionization process.

Strong-field molecular ionization plays an important role in the generation of attosecond pulses and electron wave packets [1–4]. It can also be used to track excited state molecular dynamics and for molecular imaging [5–10]. A detailed understanding of the ionization dynamics is crucial for developing these frontier areas of molecular science [11]. In particular, with a push to improve time resolution in molecular dynamics experiments [12, 13], generate multi-hole electron wave packets [14–18] and single attosecond pulses, it is important to understand how ionization depends on the duration of the strong-field driving pulse [19, 20]. Here, we study strong-field molecular ionization as a function of pulse duration, going from several tens of fs to below 10 fs, where vibrational dynamics is frozen out (the ‘impulsive limit’) [21]. Surprisingly, we find that as we shorten the pulse duration from about 40 fs to less than 10 fs, there is a dramatic change in the photoelectron spectrum, which reflects a change in the combination of ionic continua that are accessed during the ionization process. We observe similar behavior in three different molecules ( $\text{CH}_2\text{I}Br$ ,  $\text{CH}_2\text{BrCl}$  and  $\text{C}_6\text{H}_5\text{I}$ ) and demonstrate that the result depends more sensitively on pulse duration than spectral content. For  $\text{CH}_2\text{I}Br$ , we further interpret the experimental measurements in terms of calculations of strong-field molecular ionization which include vibrational dynamics on intermediate neutral states during the ionization process.

Our experimental apparatus consists of an amplified Ti:sapphire laser system, which produces 30 fs pulses with an energy of 1 mJ and a central wavelength of 780 nm. The pulses are focused into an Argon gas cell to create a filament and broaden the spectrum [22]. The pulses are compressed to near the transform limit with a 4-f grating compressor, and measured using a Self-Diffraction (SD) FROG apparatus [23]. The broadest spectrum we produce is capable of supporting sub 6 fs

pulses, and FROG measurements place an upper limit on the duration of the full bandwidth pulses of about 8-9 fs. The spectrum is cut using a variable slit in the grating compressor in order to obtain the variable bandwidth for the measurements below. The spectrum of the pulse is adjusted at the focusing element instead of the Fourier plane in order to avoid hard cutoffs at the edges of the spectrum, which would lead to a structured pulse in the time domain.

The linearly polarized laser beam crosses an effusive molecular beam in a vacuum chamber. Here we generate electrons and ions, which are detected by accelerating them toward a dual stack of microchannel plates and phosphor screen with an electrostatic lens configured for velocity map imaging (VMI). The VMI lens produces a two-dimensional projection of the three-dimensional charged particle velocity distribution [24]. The hit locations on the phosphor screen from each laser shot are recorded and digitized by a CMOS camera which reads them into memory as separate images. The laser intensity is adjusted between 10-13 TW/cm<sup>2</sup> to keep the ionization yield roughly constant as the pulse duration is varied, yielding about 20±10 electrons per laser shot. A computer algorithm extracts the hit locations from each image and synthesizes a single data image for any given laser pulse parametrization. This image is inverse-Abel transformed with the BASEX method [27] and converted to a photoelectron spectrum. We focus on the yield that is generated ±30° around the laser polarization direction. Integrating over all angles yields similar results, with slightly less contrast of the peaks.

Figure 1 shows photoelectron spectra for  $\text{CH}_2\text{I}Br$  as a function of pulse duration. For longer pulses (>20 fs), two peaks are visible: one at ≈1.2 eV and the other at ≈0.7 eV. Earlier work assigned these peaks to leaving the molecule in the first two states of the molecular cation:  $D_0$  and  $D_1$ , respectively. The assignment of the spec-

trum to the molecular ions was verified using electron-ion coincidence spectroscopy [25]. While the yield from 0-0.2 eV and around 1.6 eV can be assigned to  $D_2/D_3$  [25], we focus on the yield to  $D_0$  and  $D_1$  for simplicity here. Earlier work [28] also established that these peaks involve resonance enhancement via intermediate neutral states that Stark shift into resonance during the ionization process [29]. For longer pulses, ionization proceeds such that  $D_0$  and  $D_1$  are populated with roughly equal probability. However, as the pulse is shortened to below 12 fs, the yield for the  $D_0$  peak diminishes and eventually becomes negligible compared to that of the  $D_1$  peak. This is surprising given that the ionization potential for  $D_0$  (9.7 eV) is lower than for  $D_1$  (10.2 eV) [25], and that the bandwidth of a shorter pulse is broader.

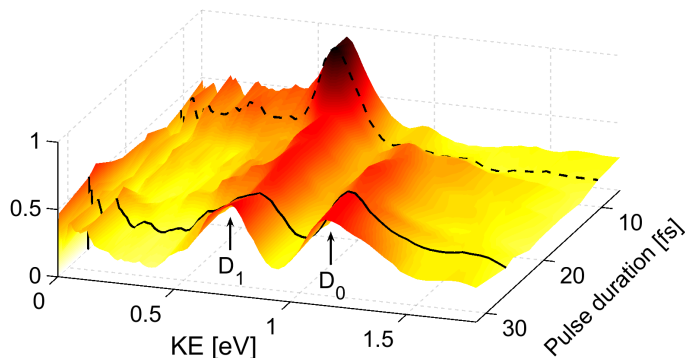


FIG. 1. (color online) Photoelectron spectra (yield vs photoelectron kinetic energy, KE) for ionization of  $\text{CH}_2\text{IBr}$  for different pulse durations.

We carried out similar measurements for other molecules and observed similar dynamics. Figure 2 shows the  $D_1$  and  $D_0$  ratio as a function of pulse duration for three different molecules:  $\text{CH}_2\text{IBr}$ ,  $\text{CH}_2\text{BrCl}$  and  $\text{C}_6\text{H}_5\text{I}$ . As the figure illustrates, all three molecules show similar behavior as a function of pulse duration. A shaded vertical bar marks the impulsive limit, corresponding to the C-H stretch vibrational period ( $\approx 11$  fs - the shortest vibrational period for organic molecules) [30].

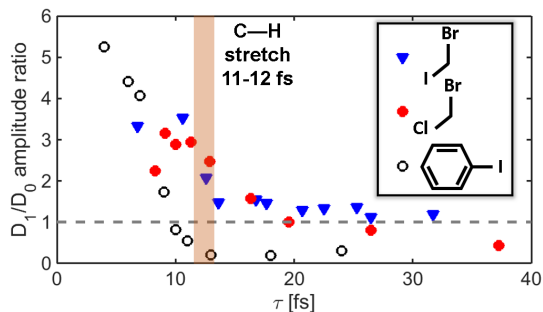


FIG. 2. (color online) Ratio of  $D_1/D_0$  as a function of pulse duration  $\tau$  for three different molecules.

We now aim to interpret the measurements and de-

termine whether the mechanism underlying the switching/control is driven by dynamics or spectral content. Since a shorter pulse duration requires a broader spectrum, it is natural to ask whether the suppression of ionization to  $D_0$  is driven by new frequency components in the pulse, or rather by the pulse becoming shorter.

We first address this question by making measurements with a series of narrowband optical pulses with different central frequencies, adding up the photoelectron spectra with the appropriate weights and comparing the result with the photoelectron spectrum measured for a short pulse that includes all the spectral components coherently. This idea is illustrated in figure 3. The top panel shows the optical spectrum of the short pulse and the weighted sum of the narrow optical spectra together, while the lower panel shows the resulting photoelectron spectra - one curve for the sum of the photoelectron spectra produced with narrowband pulses, and one curve for the photoelectron spectrum produced by a broadband pulse. The photoelectron spectra for the narrowband pulses were added in proportion to the coefficients for the narrowband optical spectra in forming the broadband spectrum as a linear combination. While the optical spectra are almost identical, there are significant differences between the two photoelectron spectra, indicating that it is not a single frequency in the pulse spectrum which drives the switching between ionic continua.

A second test that we performed was to vary the pulse duration while keeping the spectral content the same. This can be accomplished by placing a second-order spectral phase (chirp) on the broadband pulse, while varying the pulse energy to maintain a roughly constant yield. These results (to be presented in a forthcoming publication [31]) showed that the suppression of  $D_0$  only takes place for a short pulse, corroborating the conclusion drawn above.

The observations described above suggest that there is some molecular dynamics which leads to both ionic states being populated, and if the pulse is shorter than the timescale for this dynamics, then only a single ionic state is populated. As the photoelectron spectrum is determined at the moment the electron is born in the continuum (i.e. it is not affected by possible subsequent dynamics in the molecular cation), we argue that the dynamics leading to the selectivity must be neutral dynamics, involving an excited neutral state en route to the ionization continuum. As in earlier work which established the importance of dynamically Stark-shifted resonances [32–34] in strong-field molecular ionization [25, 34, 35], our current intensity and wavelength dependent measurements indicate that neutral Rydberg states Stark shift into resonance during the ionization process. The correlation between a neutral Rydberg state and low lying states of the molecular cation is typically large for only

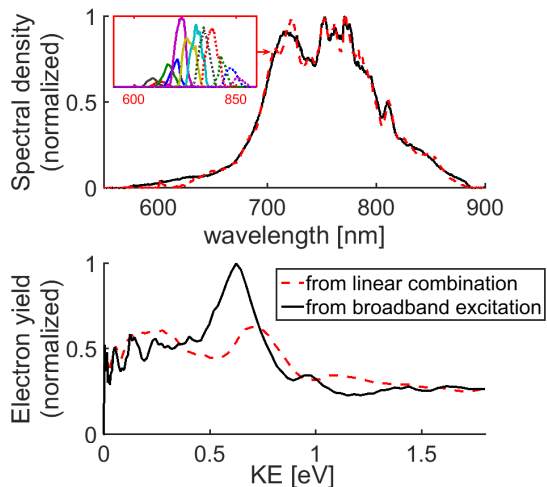


FIG. 3. (color online) Top panel: Optical spectra for broadband pulse (solid black line) and the result of summing narrowband spectra (dashed red line). Bottom panel: photoelectron spectra of  $\text{CH}_2\text{IBr}$  acquired with full bandwidth optical spectrum (solid black line), and the result of forming a linear combination of photoelectron spectra each acquired with narrowband optical excitation (dashed red line). The latter are added in proportion to their spectral weights as shown in the inset and described in the text.

a single cationic state with a similar configuration of the core - i.e. the Dyson norm for a given neutral state is large for a single low lying state of the cation, and close to zero for other states [36]. While Dyson correlations can be poor for low lying neutral states in strong-field ionization, they are better for higher lying states of the neutral where the electron which is removed during ionization does not interact with the ionic core very much and does not modify the core configuration. This means that once an intermediate neutral Rydberg state comes into resonance, it typically couples to a single ionic continuum [35]. Thus, for resonance-enhanced ionization to multiple continua, as is the case for a  $\approx 40$  fs pulse, multiple intermediate states must be involved in the ionization dynamics.

Our earlier work considered resonance enhanced ionization with separate uncoupled intermediate states for each ionization continua [35]. We extend this model to include coupling between the intermediate states, as our new measurements suggest that separate uncoupled intermediate resonances cannot account for the pulse duration dependence we observe. If the bandwidth associated with different pulse durations were to select between different independent resonances, then one would expect to find a single ionic continuum favored for a long pulse (narrow bandwidth) rather than for a short pulse (broad bandwidth), since a shorter pulse contains a larger bandwidth, which would provide less selectivity between separate resonances. Furthermore, frequency-dependent measurements of the ionization yield such as the ones il-

lustrated in figure 3 indicate that when there is resonance enhancement of the ionization yield, then it is through a single neutral state correlated with  $D_1$ . These measurements are discussed in detail in a separate publication [31].

While in principle both laser-driven resonance [6] and non-adiabatic dynamics could be responsible for coupling excited states, given the frequency-dependent measurements shown in figure 3, and motivated by earlier work [37], we focus on non-adiabatic dynamics as an explanation for the measurements shown in figures 1 and 2. We carry out calculations for  $\text{CH}_2\text{IBr}$  that include non-adiabatic coupling between excited states which support the idea that molecular dynamics drives the switching between continua as a function of pulse duration.

Before modeling the strong-field ionization with numerical integration of the time-dependent Schrödinger equation (TDSE), we carry out *ab initio* electronic structure calculations at the MS-CASPT2 level of theory [38] in order to determine which electronic states play a crucial role in the ionization process. Details on the electronic structure calculations are given in the supplementary information. The strong field ionization simulations are based on a simple model [28] which includes Stark shifted intermediate neutral resonances. This model is now extended to include vibrational dynamics and non-adiabatic coupling between multiple intermediate neutral states, as considered in earlier calculations for weak (perturbative) laser fields [37]. We focus on  $\text{CH}_2\text{IBr}$ , for which we made the most detailed measurements and calculations.

As prior measurements suggest that resonance enhancement occurs at the five-photon level [28], we considered Rydberg states ( $R_0$ ,  $R_1$  and  $R_3$ )  $\approx 8$  eV above the ground state which are correlated (i.e. similar electronic configurations) with the low-lying ionic states ( $D_0$ ,  $D_1$  and  $D_3$ ), and whose coordinate dependence follows those of the ionic states with which they are correlated. We then considered whether any nuclear coordinates led to coupling between these states. While the potential energy curves of the Rydberg states around 8 eV are largely parallel as a function of most vibrational coordinates, we found one mode ( $\text{CH}_2$  wagging) along which motion leads to degeneracy (and therefore to population transfer via non-adiabatic coupling) between states correlated with  $D_0$ ,  $D_1$  and  $D_3$ . The potential energy curves of these states along this normal mode coordinate are shown in Figure 4. In our calculations, population excited to  $R_1$  (which based on experimental measurements is most strongly coupled to  $S_0$  via the laser [31]) can quickly relax to  $R_3$  and  $R_0$  via rapid nuclear dynamics and non-adiabatic coupling. Based upon matches of the computed energy differences and similarities between electronic configurations of the electronic configurations,  $R_0$ ,  $R_1$  and  $R_3$  are coupled to  $D_0$ ,  $D_1$  and  $D_3$  respectively. The strong-field ionization calculations produced

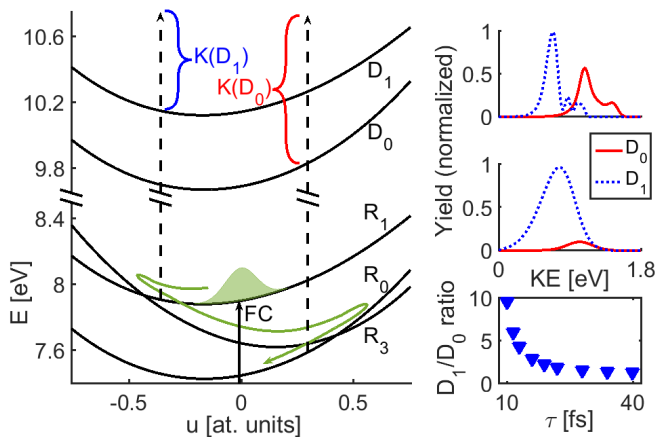


FIG. 4. (color online) Left panel: calculated potential energy surfaces for  $\text{CH}_2\text{IBr}$  along the  $\text{CH}_2$  wagging mode. FC: Franck-Condon point for excitation from the minimum of  $S_0$  ( $u=0$ ). Upper right panel: calculated photoelectron spectra for 40 fs pulse. Middle right panel: calculated photoelectron spectra for 10 fs pulse. Bottom right panel: calculated  $D_1/D_0$  yield ratio as a function of pulse duration  $\tau$ .

the photoelectron spectrum as a function of pulse duration, as in the measurements. The energies of the resonant intermediate states were based on the electronic structure calculations and comparison with experimental spectra. Laser parameters, such as the intensity, central frequency and pulse duration, were based on experimental parameters. The coupling strengths (multiphoton Rabi frequencies) are given in the supplementary material.

As the  $S_0 \rightarrow R_1$  resonance dominates, population is initially transferred from  $S_0$  to  $R_1$ . As figure 4 illustrates, motion along the  $\text{CH}_2$  wagging mode couples states  $R_0$ ,  $R_1$  and  $R_3$ . The Franck Condon point (minimum of  $S_0$ ) is close to the  $R_1/R_3$  crossing, leading to rapid population transfer from  $R_1$  to  $R_3$  ( $\approx 5$  fs). Within  $\approx 10$  fs the wave packet on  $R_3$  can proceed to the  $R_3/R_0$  crossing. Thus, for a long pulse, ionization can proceed to a mixture of the ionic states  $D_0$ ,  $D_1$  and  $D_3$  coupled with the three neutral states  $R_0$ ,  $R_1$  and  $R_3$ . While our measurements show evidence of ionization to all three of these states, we concentrate on the competition between  $D_0$  and  $D_1$  because the measurements are cleanest for these states. In the limit of a short laser pulse, one might expect  $D_1$  (which is correlated with  $R_1$ ) to dominate the ionization yield, since  $R_1$  can shift into resonance and there is not sufficient time for the wave packet to move away from the FC on  $R_1$  during the ionization. The ionization calculations aimed to test this hypothesis.

As the top right and middle panels of figure 4 illustrate, the photoelectron spectrum for a long pulse (40 fs) shows peaks corresponding to  $D_0$  and  $D_1$ , whereas the photoelectron spectrum for a 10 fs pulse shows a single

peak corresponding to  $D_1$  only. This is in agreement with the results shown in figure 1, which shows two peaks corresponding to  $D_1$  and  $D_0$  for a long pulse and a single peak corresponding to  $D_1$  for a short pulse. The bottom right panel shows a decreasing  $D_1/D_0$  ratio as a function of pulse duration, in agreement with the results shown in figure 2. One aspect of the measurements which is not reflected in the calculations is the width of the peaks in the PES as a function of pulse duration. The measurements show relatively narrow peaks for both short and long pulse durations, while the calculations show peaks which broaden as a function of decreasing pulse duration.

Our interpretation of the pulse duration dependence relies on neutral state resonances enhancing the ionization yield. Thus one would expect that there is no change in the ionization yield for different ionic continua with pulse duration if there are no important resonances. In order to test this, we performed measurements of the photoelectron spectrum vs pulse duration in  $\text{CS}_2$ , for intensities where there are no intermediate resonances for our laser frequency. We also performed measurements in  $\text{CH}_2\text{IBr}$  for very low intensities where the intermediate states do not Stark shift into resonance. In both cases we found that the photoelectron spectrum did not change substantially with pulse duration, as one would expect based on our interpretation which relies on dynamics in intermediate neutral states.

In conclusion, we study the state-resolved ionization yield as a function of pulse duration for several molecules and find that for relatively long pulses, vibrational dynamics and non-adiabatic coupling between resonant intermediate states play an important role. For impulsive ionization with pulses less than 10 fs in duration, vibrational dynamics is frozen and no longer plays an important role in the ionization process. The transition between the two regimes is clearly visible in the photoelectron spectrum, in which a dramatic switching between single and multiple continua is observed. Surprisingly, resonance-enhanced ionization plays an important role for even the shortest pulses, containing nearly an octave optical bandwidth. Our results suggest that these considerations should be relevant for a broad range of molecules in strong laser fields.

This work has been supported by the National Science Foundation under award number 1205397 and the Austrian Science Fund (FWF) through project P25827. Support from the European XLIC COST Action 1204 is also acknowledged.

- 
- [1] J. Levesque and P. B. Corkum, Canadian Journal of Physics **84**, 1 (2006), ISSN 0008-4204.
  - [2] M. Krug, T. Bayer, M. Wollenhaupt, C. Sarpe-Tudoran, T. Baumert, S. S. Ivanov, and N. V. Vitanov, New Journal of Physics **11**, 105051 (2009).

- [3] P. Agostini and L. F. DiMauro, Reports on progress in physics **67**, 813 (2004).
- [4] E. Goulielmakis, Z.-H. Loh, A. Wirth, R. Santra, N. Rohringer, V. S. Yakovlev, S. Zherebtsov, T. Pfeifer, A. M. Azzeer, M. F. Kling, et al., Nature **466**, 739 (2010).
- [5] T. Baumert, V. Engel, C. Meier, and G. Gerber, Chemical Physics Letters **200**, 488 (1992), ISSN 0009-2614.
- [6] D. Irimia and M. H. M. Janssen, Journal of Chemical Physics **132**, 234302 (2010), ISSN 00219606.
- [7] J. L. Hansen, H. Stapelfeldt, D. Dimitrovski, M. Abu-samha, C. P. J. Martiny, and L. B. Madsen, Phys. Rev. Lett. **106**, 073001 (2011).
- [8] D. Villeneuve, H. Niikura, N. Milosevic, T. Brabec, and P. Corkum, Nuclear Instruments and Methods in Physics Research Section B: Beam Interactions with Materials and Atoms **241**, 69 (2005), ISSN 0168-583X, the Application of Accelerators in Research and Industry - Proceedings of the Eighteenth International Conference on the Application of Accelerators in Research and Industry (CAARI 2004).
- [9] M. Meckel, D. Comtois, D. Zeidler, A. Staudte, D. Pavičić, H. C. Bandulet, H. Pépin, J. C. Kieffer, R. Dörner, D. M. Villeneuve, et al., Science **320**, 1478 (2008).
- [10] W. Li, A. A. Jaroń-Becker, C. W. Hogle, V. Sharma, X. Zhou, A. Becker, H. C. Kapteyn, and M. M. Murnane, Proceedings of the National Academy of Sciences **107**, 20219 (2010), <http://www.pnas.org/content/107/47/20219.full.pdf>.
- [11] M. Ivanov and O. Smirnova, Phys. Rev. Lett. **107**, 213605 (2011).
- [12] A. Baltuška, T. Udem, M. Uiberacker, M. Hentschel, E. Goulielmakis, C. Gohle, R. Holzwarth, V. S. Yakovlev, A. Scrinzi, T. W. Hänsch, et al., Nature **421**, 611 (2003), ISSN 0028-0836.
- [13] P. Reckenthaeler, M. Centurion, W. Fuß, S. A. Trushin, F. Krausz, and E. E. Fill, Phys. Rev. Lett. **102**, 213001 (2009).
- [14] S. V. Menon, J. P. Nibarger, and G. N. Gibson, Journal of Physics B: Atomic, Molecular and Optical Physics **35**, 2961 (2002).
- [15] P. Johnsson, R. López-Martens, S. Kazamias, J. Mauritsson, C. Valentin, T. Remetter, K. Varjú, M. B. Gaarde, Y. Mairesse, H. Wabnitz, et al., Phys. Rev. Lett. **95**, 013001 (2005).
- [16] M. F. Kling, C. Siedschlag, A. J. Verhoef, J. I. Khan, M. Schultze, T. Uphues, Y. Ni, M. Uiberacker, M. Drescher, F. Krausz, et al., Science **312**, 246 (2006).
- [17] B. K. McFarland, J. P. Farrell, P. H. Bucksbaum, and M. Gühr, Science **322**, 1232 (2008).
- [18] B. Bergues, M. Kübel, N. G. Johnson, B. Fischer, N. Camus, K. J. Betsch, O. Herrwerth, A. Senfleben, A. M. Saylor, T. Rathje, et al., Nature communications **3**, 813 (2012).
- [19] G. Sansone, E. Benedetti, F. Calegari, C. Vozzi, L. Avaldi, R. Flammini, L. Poletto, P. Villoresi, C. Altucci, R. Velotta, et al., Science **314**, 443 (2006).
- [20] M.-C. Chen, C. Mancuso, C. Hernández-García, F. Dolar, B. Galloway, D. Popmintchev, P.-C. Huang, B. Walker, L. Plaja, A. A. Jaroń-Becker, et al., Proceedings of the National Academy of Sciences **111**, E2361 (2014).
- [21] X. Xie, E. Lötstedt, S. Roither, M. Schöffler, D. Kartashov, K. Midorikawa, A. Baltuška, K. Yamanouchi, and M. Kitzler, Scientific Reports **5** (2015), article.
- [22] G. Stibenz, N. Zhavoronkov, and G. Steinmeyer, Optics letters **31**, 274 (2006).
- [23] R. Trebino, K. W. DeLong, D. N. Fittinghoff, J. N. Sweetser, M. A. Krumbügel, B. A. Richman, and D. J. Kane, Review of Scientific Instruments **68**, 3277 (1997).
- [24] A. T. J. B. Eppink and D. H. Parker, Review of Scientific Instruments **68**, 3477 (1997).
- [25] P. Sándor, A. Zhao, T. Rozgonyi, and T. Weinacht, Journal of Physics B: Atomic, Molecular and Optical Physics **47**, 124021 (2014).
- [26] A. E. Boguslavskiy, J. Mikosch, A. Gijsbertsen, M. Spanner, S. Patchkovskii, N. Gador, M. J. J. Vrakking, and A. Stolow, Science **335**, 1336 (2012).
- [27] V. Dribinski, A. Ossadtchi, V. A. Mandelshtam, and H. Reisler, Review of Scientific Instruments **73**, 2634 (2002).
- [28] W. D. M. Lunden, P. Sándor, T. C. Weinacht, and T. Rozgonyi, Phys. Rev. A **89**, 053403 (2014).
- [29] Note1, we note that intermediate neutral states can play an important role even for very short pulses, where the resonance condition is only met for a relatively short time, provided that there is sufficiently strong coupling.
- [30] Y. Yu, K. Lin, X. Zhou, H. Wang, S. Liu, and X. Ma, The Journal of Physical Chemistry C **111**, 8971 (2007).
- [31] V. Tagliamonti, P. Sándor, A. Zhao, T. Rozgonyi, and T. Weinacht (In preparation).
- [32] G. N. Gibson, R. R. Freeman, T. J. McIlrath, and H. G. Muller, Phys. Rev. A **49**, 3870 (1994).
- [33] R. R. Freeman, P. H. Bucksbaum, H. Milchberg, S. Darack, D. Schumacher, and M. E. Geusic, Phys. Rev. Lett. **59**, 1092 (1987).
- [34] G. N. Gibson, R. R. Freeman, and T. J. McIlrath, Phys. Rev. Lett. **69**, 1904 (1992).
- [35] W. D. M. Lunden, D. Geißler, P. Sándor, T. C. Weinacht, and T. Rozgonyi, Phys. Rev. A **89**, 053404 (2014).
- [36] M. Spanner, S. Patchkovskii, C. Zhou, S. Matsika, M. Kottur, and T. C. Weinacht, Phys. Rev. A **86**, 053406 (2012).
- [37] M. Seel and W. Domcke, The Journal of Chemical Physics **95**, 7806 (1991).
- [38] J. Finley, P.-A. Malmqvist, B. O. Roos, and L. Serrano-Andrés, Chem. Phys. Lett. **288**, 2223 (1989).
- [39] See Supplemental Material [url], which includes Refs. [40-55].
- [40] R. Trebino, K. W. DeLong, D. Fittinghoff, et al., *Review of Scientific Instruments*, **68**, 3277, (1997).
- [41] M. J. Frisch, G. W. Trucks and H. B. Schlegel et al., GAUSSIAN 2003, Gaussian Inc., Wallingford, CT, (2003).
- [42] P. J. Stephens, F. J. Devlin, C. F. Chabalowski and M. J. Frisch, *J. Phys. Chem.* **98**, 11623, (1994).
- [43] K. A. Peterson, D. Figgen, E. Goll, H. Stoll and M. Dolg, *J. Chem. Phys.*, **119**, 11113, (2003).
- [44] J. González-Vázquez, L. González, S.R. Nichols, T.C. Weinacht and T. Rozgonyi, *Phys.Chem.Chem.Phys.* **93**, (2010)
- [45] J. Finley, P.-A. Malmqvist, B.O. Roos, L. Serrano-Andrés, *Chem. Phys. Lett.*, **288**, 299, (1998). K. Andersson, P.-A. Malmqvist, B.O. Roos, *J. Chem. Phys.*, **96**, 1218, (1992).
- [46] F. Aquilante, L. De Vico, N. Ferré, G. Ghigo, P.-A. Malmqvist, P. Neogrády, T.B. Pedersen, M. Pitonak, M. Reiher, B.O. Roos, L. Serrano-Andrés, M. Urban, V. Veryazov, R. Lindh, *J. Comput. Chem.* **31**, 224-247,

- (2010)
- [47] M. Reiher, *Theor. Chem. Acc.*, **116**, 241252, (2006).
- [48] P.-O. Widmark, P.-A. Malmqvist and B. O. Roos, *Theor. Chim. Acta*, **77**, 291, (1990). B. O. Roos, R. Lindh, P.-A. Malmqvist, V. Veryazov and P.-O. Widmark, *J. Phys. Chem. A*, **108**, 28512858, (2004).
- [49] K. Kaufmann, W. Baumeiter and M. Jungen, *J. Phys. B*, **22**, 223-2240, (1989).
- [50] C.M.Marian and U.Wahlgern, *Chem. Phys. Lett.*, **251**, 357, (1996).
- [51] A.F. Lago, J.P. Kercher, A. Bödi, B. Sztáray, B. Miller, D. Wurzelmann and T. Baer, *J. Phys. Chem. A*, **109**, 1802, (2005).
- [52] Penner and Amirav *J. Chem. Phys.*, **93**, 8556, (1990).
- [53] M. Seel and W. Domcke, *J. Chem. Phys.*, **95**, 7806, (1991). T. Rozgonyi, A. Glass and T. Feurer, *J. Appl. Phys.*, **88**, 2936, (2000).
- [54] C. Trallero-Herrero, D. Cardoza, T.C. Weinacht and J.L. Cohen, *Phys. Rev. A*, **71**, 013423, (2005).
- [55] W. Lunden, P. Sándor, T.C. Weinacht and T. Rozgonyi, *Phys. Rev. A*, **89**, 053403, (2014).